Research Article Vol. 12, No. 11 / November 2024 / Photonics Research 2741

PHOTONICS Research

Reducing statistical noise in frequency ratio measurement between Ca^+ and Sr optical clocks with a frequency-synthesized local oscillator from a Sr optical clock

Haosen Shi,[1,†] Bingkun Lu,[2,3,4,†] Huaqing Zhang,[5,6,†] Ruming Hu,[5,6,7] Yuan Qian,[5,6,7] Yao Huang,[5,6] Tao Yang,[2,4] Yuan Yao,[1] Hongfu Yu,[1] Zhanjun Fang,[2,4] Kelin Gao,[5,6] Hua Guan,[5,6,8,9] Yige Lin,[2,4,10] Yanyi Jiang,[1,11] and Longsheng Ma[1]

[1]State Key Laboratory of Precision Spectroscopy, East China Normal University, Shanghai 200062, China
[2]Division of Time and Frequency Metrology, National Institute of Metrology, Beijing 100029, China
[3]Key Laboratory of Atomic Frequency Standards, Innovation Academy for Precision Measurement Science and Technology, Chinese Academy of Sciences, Wuhan 430071, China
[4]Key Laboratory of State Administration for Market Regulation (Time Frequency and Gravity Primary Standard), Beijing 100029, China
[5]Innovation Academy for Precision Measurement Science and Technology, Chinese Academy of Sciences, Wuhan 430071, China
[6]Department of Precision Instrument, Tsinghua University, Beijing 100084, China
[7]University of Chinese Academy of Sciences, Beijing 100049, China
[8]Wuhan Institute of Quantum Technology, Wuhan 430206, China
[9]e-mail: guanhua@apm.ac.cn
[10]e-mail: linyige@nim.ac.cn
[11]e-mail: yyjiang@phy.ecnu.edu.cn
[†]These authors contributed equally to this work.

Received 20 August 2024; revised 18 September 2024; accepted 22 September 2024; posted 23 September 2024 (Doc. ID 539892); published 1 November 2024

Optical frequency ratio measurement between optical atomic clocks is essential to precision measurement as well as the redefinition of the second. Currently, the statistical noise in frequency ratio measurement of most ion clocks is limited by the frequency instability of ion clocks. In this work, we reduce the statistical noise in the frequency ratio measurement between a transportable Ca^+ optical clock and a Sr optical lattice clock down to $2.2 \times 10^{-15}/\sqrt{\tau}$. The local oscillator of the Ca^+ optical clock is frequency-synthesized from the Sr optical lattice clock, enabling a longer probe time for Ca^+ clock transition. Compared to previous measurement using independent local oscillators, we achieve 10-fold reduction in comparison campaign duration. © 2024 Chinese Laser Press

https://doi.org/10.1364/PRJ.539892

1. INTRODUCTION

Optical atomic clocks have reached a systematic frequency uncertainty at the 10^{-18} level and even beyond [1–8]. The unprecedented accuracy and precision make optical clocks indispensable tools in time and frequency metrology. In metrology, a new definition of International System of Units (SI) second based on optical transitions has been proposed [9]. Meanwhile, optical clocks are now popular in precision measurement and tests of fundamental physics [10,11], such as the search for dark matter [12], testing the possible variance of fundamental physical constants [13,14], and chronometric geodesy [2,15]. To realize above applications, frequency comparison or frequency ratio measurement between optical clocks is required. Since statistical noise determines measurement precision as well as statistical uncertainty in frequency ratio measurement, low statistical noise is pursued, especially in applications with limited observation time and those demanding high accuracy.

As the noise induced by state-of-the-art optical frequency combs is below 1×10^{-17} at 1 s averaging time [16–18], statistical noise in frequency ratio measurement between independent optical clocks is mostly determined by the frequency instability of the clocks. Nowadays, the frequency stability of optical clocks is mostly determined by the frequency noise of their local oscillators (LOs). First, laser frequency noise leads to a limited laser-atomic probe time T_p, which sets a quantum projection noise (QPN)-limited fractional frequency instability of

$$\sigma_{\mathrm{QPN}}(\tau) \propto \frac{1}{\nu_c T_p}\sqrt{\frac{T_c}{N\tau}}, \tag{1}$$

where ν_c, τ, T_c, and N are the transition frequency, averaging time, cycle time, and number of unentangled atoms, respectively [19]. Second, the frequency stability of clocks also suffers from the LO frequency noise through the Dick effect [20] when LO interacts with the atoms intermittently. As a result, a long probe time is preferred to increase the interrogation duty cycle (T_p/T_c) to reduce the Dick noise.

Compared to optical lattice clocks operating with 10^3–10^4 atoms, single ion clocks exhibit inferior frequency stability, which is predominantly influenced by QPN. To reduce the QPN limit of ion clocks, LOs with high frequency stability have been developed to increase the probe time. For example, the frequency instability of a Yb^+ optical clock was improved from $5\times10^{-15}/\sqrt{\tau}$ [21] to $1\times10^{-15}/\sqrt{\tau}$ [22] by using an ultra-stable laser frequency-stabilized to a cryogenic silicon cavity [23] instead of a room-temperature ultra-low expansion (ULE) optical cavity. By improving the frequency stability of ion clocks, the statistical noise reaches $1.3\times10^{-15}/\sqrt{\tau}$ in frequency ratio measurement between Al^+ and Yb clocks [24] and $1\times10^{-15}/\sqrt{\tau}$ between Yb^+ and Sr clocks [25]. Alternatively, pre-stabilizing LOs with multiple atomic ensembles has also been proposed to elongate the probe time [26–28].

Except for improving the clock stability, various protocols have been adopted to reduce the statistical noise in frequency comparisons between optical clocks. Synchronous interrogation of clock transitions with phase-coherent LOs can minimize the Dick noise by common-mode cancelation of laser frequency noise-induced excitation rate fluctuation [3,29–31]. A statistical noise of $5\times10^{-17}/\sqrt{\tau}$ in the frequency ratio measurement between two Sr clocks was achieved, approaching the QPN limit [3]. Based on synchronous interrogation, correlation spectroscopy uses a protocol to obtain atom–atom frequency measurement that is independent of laser frequency noise. It can further extend the probe time beyond the LO coherence time [32], and thereby it reduces the QPN limit. Differential spectroscopy extends the LO coherence time: after two phase-coherent LOs synchronously interrogating two atomic species, the spectrum of one atomic species is used to correct the LO frequency noise before interrogating the other atomic species again [33–35]. With a combination of differential spectroscopy and a zero-dead-time optical clock using two atomic-ensembles, a statistical noise of $2\times10^{-16}/\sqrt{\tau}$ in the frequency ratio measurement between Al^+ and Yb clocks was achieved [35]. The above schemes rely on synchronous interrogation between two optical clocks.

Here in the frequency ratio measurement between a transportable Ca^+ optical clock [36] and a Sr optical lattice clock [37], the timing sequences of the two optical clocks are quite different. Thus, the above schemes cannot be applied in this measurement. Instead, we extend the LO coherence time of the Ca^+ clock by frequency-synthesizing from the Sr clock with an optical frequency divider (OFD) [18]. In addition to the phase coherence transfer from the Sr optical lattice clock to the LO of the Ca^+ optical clock at 729 nm, the OFD directly enables the measurement of the frequency ratio between the two optical clocks, which are both the secondary representations of the SI second [38]. Compared to previous measurement using independent LOs, the method used in this work improves the statistical noise by a factor of 3.2, reaching $2.2\times10^{-15}/\sqrt{\tau}$. As a result, it enables a 10-fold reduction of the comparison campaign duration to a certain statistical uncertainty. Moreover, when the LO of the Ca^+ optical clock is frequency-synthesized from the Sr clock, a Rabi spectrum with 1.6 Hz linewidth is obtained, the narrowest linewidth of the Ca^+ clock to the best of our knowledge.

2. EXPERIMENTAL SETUP

In this work, an OFD built by East China Normal University (ECNU) and a transportable Ca^+ clock built by Innovation Academy for Precision Measurement Science and Technology (APM) were transported to National Institute of Metrology (NIM) of China to compare against a Sr optical lattice clock there. The detailed setups of the OFD, Ca^+ clock, and Sr clock are introduced elsewhere [18,36,37].

The operation timing sequences for the Ca^+ and Sr clocks are shown in Figs. 1(a) and 1(b), respectively. For the Ca^+ clock, after Doppler cooling, the ion is pumped to either $|^2S_{1/2}, m_j=\pm1/2\rangle$ state for clock interrogation. The total dead time for a single cycle is ~20 ms. We alter the probe time T_p for different situations. The state of the ion is detected 10 times to improve the signal-to-noise ratio (SNR). In order to cancel the first-order Zeeman shift, the electric quadrupole shift, and the tensor Stark shift, three pairs of Zeeman transitions of $|^2S_{1/2}, m_j=\pm1/2\rangle \rightarrow |^2D_{5/2}, m_j=\pm1/2,\ \pm3/2,\ \pm5/2\rangle$ are used to calculate the center frequency of the Ca^+ clock transition. As a result, the clock laser frequency is steered every 120 clock cycles, i.e., ~13 s when $T_p=80$ ms. For the Sr clock, the atoms are trapped and cooled in a two-stage magneto-optical trap (MOT). Then they are loaded into a one-dimensional optical lattice and are prepared to either $|^1S_0, m_F=\pm9/2\rangle$ state. Afterwards, the atoms are probed for 200 ms. The total cycle time for the Sr clock is 1086 ms. To cancel the first-order Zeeman shift, both $|^1S_0, m_F=\pm9/2\rangle \rightarrow |^3P_0, m_F=\pm9/2\rangle$ transitions are probed to calculate the center frequency of the clock transition, which is corrected every four clock cycles (~4.3 s). As we can see in Fig. 1, the two clocks operate with distinct timing sequences. Thus it is difficult to utilize the comparison protocols such as synchronization comparison [3,29–31] or differential spectroscopy [34], where synchronized interrogation is always required.

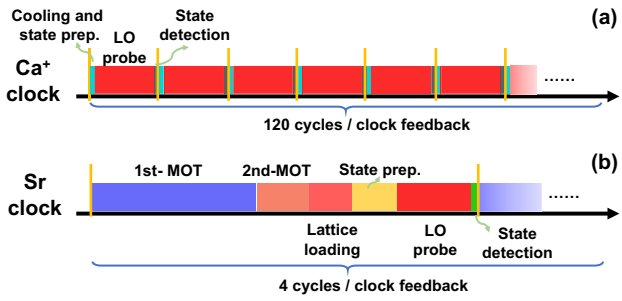

Fig. 1. Timing control sequence for (a) Ca^+ optical clock and (b) Sr optical lattice clock.

The experimental setup of the frequency ratio measurement between the two clocks is shown in Fig. 2(a). The Ca^+ and Sr clocks are placed in two separated rooms, while the cavity-stabilized LO of the Sr optical clock and the OFD are placed in a third room. For the Sr clock, the LO is a 698 nm laser frequency-stabilized to a 30-cm-long ULE optical reference cavity, yielding a frequency instability better than 3×10^{-16} at an averaging time of 1–10 s. The laser light is delivered to interact with Sr atoms, and the laser frequency is steered by an acoustic-optic modulator [AOM, AOM2 in Fig. 2(a)] to lock the laser frequency to the $^1S_0 \rightarrow {}^3P_0$ transition of Sr atoms. Meanwhile, ~2.5 mW laser light is sent to the OFD via a phase-noise-canceled fiber link, serving as the reference of the OFD. The driving frequency of AOM3 is also updated to ensure the reference frequency $\nu_{698} = \nu_{Sr}$. For the Ca^+ clock, a single frequency laser at 729 nm is used as the LO. Instead of locking its frequency ν_{729} to an independent optical reference cavity, its frequency is synthesized from the LO of the Sr clock at 698 nm by the OFD with a preset ratio R_0.

In order to obtain a high-SNR beat note between the 729 nm laser and the comb light, we use injection locking amplification [39] to amplify the 729 nm laser. Near 40 μW light from a 729 nm master laser is injected into a slave laser through an optical isolator, and the slave laser outputs 25 mW laser light with the same frequency as the master laser. After beam splitting, the laser light is coupled into a piece of phase-noise-canceled fiber. About 5 mW 729 nm light is sent to the OFD to beat against the comb light. The OFD is based on a Ti:sapphire optical frequency comb with an optical spectral coverage of 0.5–1.1 μm, and its repetition rate f_r (~1 GHz) and offset frequency f_0 are loosely locked to a hydrogen maser [40]. The transfer oscillator scheme [41] is adopted in the optical frequency division to cancel out the comb frequency noise as shown in Fig. 2(b). First, the beat signal between the 729 nm (698 nm) laser and the nearby comb line, i.e., f_{b729} (f_{b698}) is mixed with f_0 to remove the offset frequency. Then it is divided by a direct digital synthesizer (DDS) by M_1 (M_2). The divided signals are mixed, which is expressed as

$$
\begin{aligned}
f_\nu &= \frac{\nu_{729} - (f_0 + n_{729} \times f_r) + f_0}{M_1} \\
&\quad - \frac{\nu_{698} - (f_0 + n_{698} \times f_r) + f_0}{M_2} \\
&= \frac{\nu_{729} - n_{729} \times f_r}{M_1} - \frac{\nu_{698} - n_{698} \times f_r}{M_2},
\end{aligned} \tag{2}
$$

where n_{729} and n_{698} are the corresponding mode numbers of the comb lines which beat against the continuous wave lasers. When the divisors of the DDSs are set to satisfy $\frac{M_1}{M_2} = \frac{n_{729}}{n_{698}}$, the comb frequency noise is canceled out. Thus we can get a virtual beat note $f_\nu = \frac{\nu_{729}}{M_1} - \frac{\nu_{698}}{M_2}$, which is merely related to the frequencies of the 729 nm laser and the 698 nm reference laser, unconstrained by the comb frequency noise. To stabilize the frequency of the 729 nm laser, the virtual beat note is mixed with a radio frequency (RF) synthesizer at a frequency of f_{tune} to derive an error signal for feedback. The time base of the RF

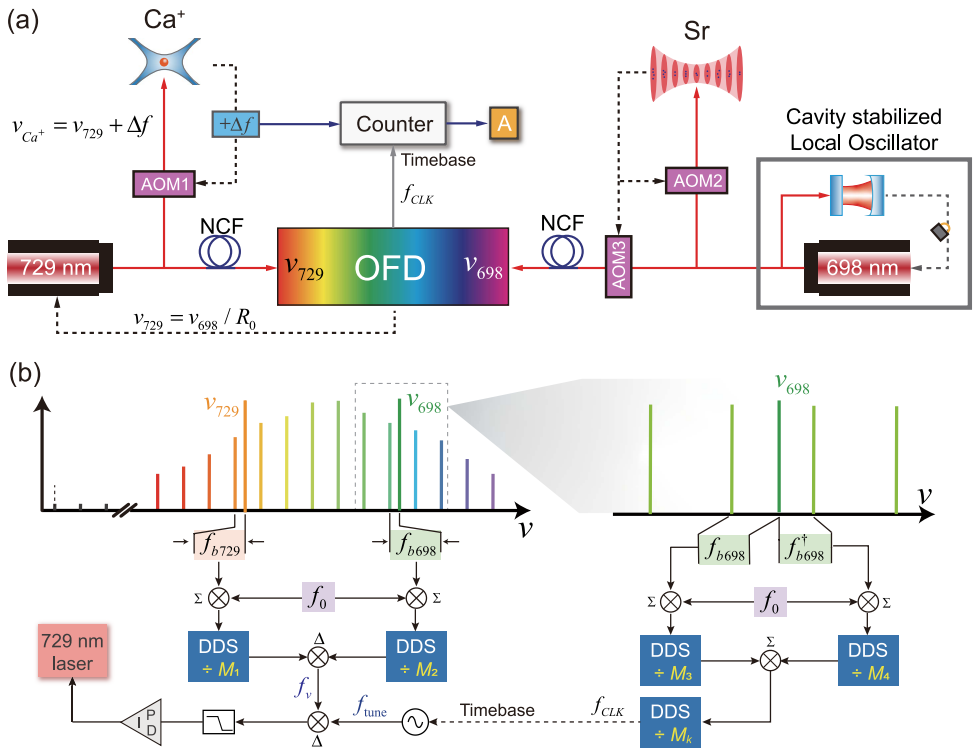

Fig. 2. (a) Schematic of the experiment setup. AOM, acoustic-optic modulator; NCF, noise canceled fiber link; DDS, direct digital synthesizer; OFD, optical frequency divider. The red straight line and the black dashed line stand for the optical path and electric control path, respectively. (b) Noise cancelation scheme for frequency noise of the comb used in OFD. The method to generate the optically referenced time base f_{CLK} is also shown on the right side.

synthesizer is an RF signal f_{CLK} at 10 MHz that is optically divided from ν_{698}. The diagram of f_{CLK} generation is shown on the right of Fig. 2(b). In this step, the beat note f_{b698} and its mirror beat note $f_{b698}^{\dagger}$ are detected, mixed with f_0, and divided in DDSs. When the divisors of the DDSs satisfy $\frac{M_3}{M_4} = \frac{n_{698}}{n_{698}+1}$, f_{CLK} can be expressed as $f_{\mathrm{CLK}} = \frac{\nu_{698}}{M_k} \times (\frac{1}{M_3} - \frac{1}{M_4})$, where the divisor M_k is used to set the signal around 10 MHz for the external time base of the RF synthesizer. Finally, the error signal $\delta = f_v - f_{\mathrm{tune}}$ is sent to a digital servo to feedback to the current of the 729 nm laser. As a result, when the servo loop is closed, the OFD links the two laser frequencies as $\nu_{729} = \nu_{698}/R_0$ with a preset ratio

$$R_0 = 1 \Big/ \left(\frac{M_1}{M_2} + \frac{f_{\mathrm{tune}}}{10^7} \times \frac{M_1}{M_k} \times \frac{M_4 - M_3}{M_3 M_4} \right). \tag{3}$$

After that, the frequency-synthesized 729 nm laser light is sent to probe the Ca^+ ion. AOM1 is used to shift laser frequency to be resonant on the $^2S_{1/2} \rightarrow {}^2D_{5/2}$ transition of Ca^+ at ν_{Ca^+}.

Using the setup shown in Fig. 2(a), we improve the frequency stability of the 729 nm laser, and meanwhile we can obtain the frequency ratio between ν_{Sr} and ν_{Ca^+} by recording the correction frequency Δf with a frequency counter referenced to the optically divided RF clock f_{CLK}. When the Sr clock is used as the OFD reference, i.e., $\nu_{698} = \nu_{\mathrm{Sr}}$, the frequency ratio between Ca^+ and Sr optical clocks can be expressed as

$$\nu_{Ca^+} = \frac{\nu_{\mathrm{Sr}}}{R_0} + \frac{A}{10^7} \times f_{\mathrm{CLK}} = \frac{\nu_{\mathrm{Sr}}}{R_0} + \frac{A}{10^7} \times \frac{\nu_{\mathrm{Sr}}}{M_k} \left(\frac{1}{M_3} - \frac{1}{M_4} \right), \tag{4}$$

where A is the counted value for Δf. As a result, the frequency ratio between the Ca^+ and Sr clocks is derived as

$$r_{Ca^+/\mathrm{Sr}} = \frac{1}{R_0} + \frac{A}{10^7} \times \frac{M_3 M_4}{M_k (M_4 - M_3)}. \tag{5}$$

3. RESULT AND DISCUSSION

Compared to the LO stabilized to a room-temperature ULE cavity at 729 nm [36], the frequency-synthesized 729 nm LO derived by the OFD has an improved frequency stability, determined by the 698 nm cavity-stabilized laser in short-term scale (within the laser servo time constant of the Sr optical clock, i.e., 17 s) and Sr atomic transition in long-term scale (>17 s) [42]. As a result, a longer probe time for Ca^+ clock is permitted. Figure 3 displays the Rabi spectra of the Ca^+ clock transition with a probe time $T_p = 160$ ms, 320 ms, and 640 ms, and spectra with a full width at half maximum (FWHM) linewidth of 4.8 Hz, 2.5 Hz, and 1.6 Hz are observed, respectively. At each frequency point, the ion is probed for 100 times to improve the SNR. Notably, for the 320 ms and 640 ms probe time, it takes 34 and 66 s in each frequency step, respectively. During this period, there is no need for linear drift compensation due to the long-term coherence of the 729 nm LO frequency-synthesized from the Sr clock. It is the narrowest linewidth for the measured Ca^+ clock transition as far as we know. Currently, the probe time is limited by the coherence time of the Ca^+ ion, ruined by magnetic field noise.

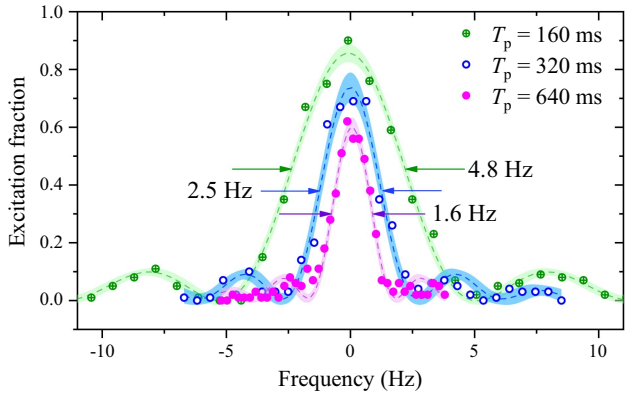

Fig. 3. Measured Rabi spectra of the Ca^+ clock transition with 100 times averaging at each frequency point. The probe time is 160 ms (green circles), 320 ms (blue circles), and 640 ms (purple dots), respectively. The dashed lines and shaded regions are the corresponding fits to the measured data using the Rabi model and their $1-\sigma$ confidence intervals.

When the probe time is increased longer than 160 ms, the magnetic field noise leads to a distortion of the spectra, which compromises the robustness of clock locking since the $|^2S_{1/2}, m_j = \pm 1/2\rangle \rightarrow |^2D_{5/2}, m_j = \pm 5/2\rangle$ transition is susceptible to magnetic field. As a result, we keep the probe time for the Ca^+ clock no longer than 160 ms to realize a robust lock during the clock comparison campaign. Figure 4 presents the statistical noise of the measured frequency ratio r with a probe time of 80 and 160 ms. Compared to previous results using independent LOs for each clock [36], the statistical noise of the measured frequency ratio is improved from $7 \times 10^{-15}/\sqrt{\tau}$ to $3.3 \times 10^{-15}/\sqrt{\tau}$ with an 80 ms probe time. Moreover, when the probe time of the Ca^+ clock is increased to 160 ms, the instability of the measured ratio is further reduced to $2.2 \times 10^{-15}/\sqrt{\tau}$. As a result, by improving the statistical noise of the measured frequency ratio, we can shorten the averaging time from 22 days to ~2 days to reach a desired statistical uncertainty of 5×10^{-18}.

As the additional instability induced by the OFD ($<8 \times 10^{-18}$ in 1–10,000 s) and the phase-noise-canceled optical fiber path (7×10^{-18}) is negligible, the measured statistical noise in Fig. 4 might be dominated by the frequency instabilities of the clocks. To estimate the independent performance of the Ca^+ clock, the LO at 729 nm is synthesized from the 698 nm cavity-stabilized laser and a time-interleaved self-comparison is carried out [29], where two locking loops with independent PIDs are employed to calculate the correction signals Δf_1 and Δf_2 for feedback to AOM1 separately. In each loop, to remove the first-order Zeeman shift, a pair of Zeeman split levels ($m_j = \pm 1/2$) is interrogated, and a correction frequency is calculated after 10 times averaging to enhance the SNR. The difference between the correction signals is recorded. The calculated overlapping Allan deviation (OADEV) gives a lower limit of its real long-term performance [29].

Figure 5 presents the calculated OADEV of a single Ca^+ clock when using Rabi spectroscopy with different

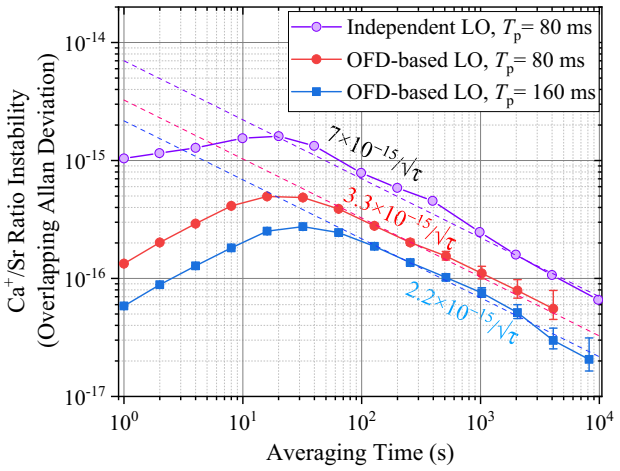

Fig. 4. Overlapping Allan deviation of the frequency ratio measurement. The LO of Ca^+ clock is frequency-synthesized from the Sr clock by OFD (red dots and blue squares for $T_p = 80$ ms and 160 ms, respectively). The dashed lines are weighted $1/\sqrt{\tau}$ fits to the measured frequency ratio data for an averaging time greater than 100 s. Error bars indicate $1-\sigma$ confidence intervals. A previous result with independent LOs for the Ca^+ and Sr clocks is shown for reference (purple circles) [36].

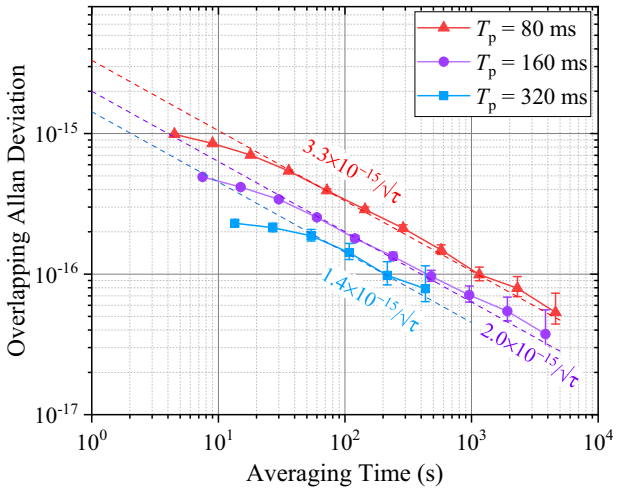

Fig. 5. Frequency instability of a single Ca^+ clock measured by the time-interleaved self-comparison method with a probe time of 80 ms (red triangles), 160 ms (purple dots), and 320 ms (blue squares). The LO of the Ca^+ clock is frequency-synthesized from the cavity-stabilized 698 nm laser with the OFD. The dashed lines are the weighted $1/\sqrt{\tau}$ fits to $T_p = 80$ ms, 160 ms, and 320 ms data for an averaging time greater than 100 s. Error bars indicate $1-\sigma$ confidence intervals.

interrogation pulse widths. For an 80 ms probe time, the frequency instability averages down following $3.3\times10^{-15}/\sqrt{\tau}$. The longer coherence time of the frequency-synthesized 729 nm LO permits an increased probe time to lower the QPN limit. The instability of the Ca^+ clock is improved to $2.0\times10^{-15}/\sqrt{\tau}$ with a 160 ms probe time. It further gets to $1.4\times10^{-15}/\sqrt{\tau}$ with a 320 ms probe time, although the remaining laser frequency drift and fluctuations of the environmental magnetic field hinder the long-term continuous locking. In each probe time, the measured instability is ~1.2 times the QPN limit, which is mainly attributed to the magnetic noise and the state preparation efficiency.

During the Ca^+/Sr clock comparison, the probe time of the Sr clock is kept at 200 ms, which gives an instability $1.18\times10^{-15}/\sqrt{\tau}$ [37]. As a result, we note that the measured statistical noise corresponds to the root sum square of uncorrelated contributions from the two clocks. The results indicate that although the OFD transfers the phase coherence from Sr to Ca^+ clock laser, the two clocks operate independently in clock comparison as no synchronous interrogation is applied due to the extinct timing control sequences for the two optical clocks. Currently, the measured statistical noise is mainly dominated by the QPN-limited frequency stability of the Ca^+ clock as well as the Dick-noise-limited frequency stability of the Sr clock. To further reduce the statistical noise in measuring the frequency ratio between Ca^+ and Sr clocks, a passive or active control of magnetic field [43] would be helpful to increase the probe time to 640 ms for the Ca^+ clock. On the other hand, it would also be achievable when two Sr atom ensembles are used in a zero-dead-time configuration to improve the frequency stability of the Sr clock.

4. CONCLUSION

In conclusion, we demonstrate a statistical noise of $2.2\times10^{-15}/\sqrt{\tau}$ in frequency ratio measurement between Ca^+ and Sr clocks using an optical frequency divider. Compared to experimental setup using independent local oscillators, the improvement on the statistical noise gives a 10-fold reduction for comparison campaign duration. As no synchronization interrogation is utilized, the statistical noise of the measured frequency ratio is determined by the frequency instabilities of the Ca^+ and Sr optical clocks, which currently are dominated by the QPN for the Ca^+ clock and Dick noise for the Sr clock, respectively.

Funding. National Natural Science Foundation of China (11927810, 11934014, 12121004, 12204494, 12320101003, 12334020, 12304548); National Key Research and Development Program of China (2021YFF0603802, 2022YFB3904001, 2022YFB3904004); State Administration for Market Regulation (CXTD202301); Natural Science Foundation of Hubei Province (2022CFA013, 2023EHA006); Youth Innovation Promotion Association of the Chinese Academy of Sciences (Y2022099); CAS Project for Young Scientists in Basic Research (YSBR-055, YSBR-085).

Acknowledgment. We thank Qunfeng Chen, Yanmei Hao, Zixiao Ma, and Baolin Zhang for the early work on the setup of the transportable Ca^+ clock.

Disclosures. The authors declare no conflicts of interest.

Data Availability. Data underlying the results presented in this paper are not publicly available at this time but may be obtained from the authors upon reasonable request.

REFERENCES

1. M. Schioppo, R. C. Brown, W. F. McGrew, *et al.*, "Ultrastable optical clock with two cold-atom ensembles," Nat. Photonics **11**, 48–52 (2017).
2. W. F. McGrew, X. Zhang, R. J. Fasano, *et al.*, "Atomic clock performance enabling geodesy below the centimetre level," Nature **564**, 87–90 (2018).
3. E. Oelker, R. B. Hutson, C. J. Kennedy, *et al.*, "Demonstration of 4.8×10^{-17} stability at 1 s for two independent optical clocks," Nat. Photonics **13**, 714–719 (2019).
4. T. Bothwell, D. Kedar, E. Oelker, *et al.*, "JILA SrI optical lattice clock with uncertainty of 2.0×10^{-18}," Metrologia **56**, 065004 (2019).
5. B. Bloom, T. Nicholson, J. Williams, *et al.*, "An optical lattice clock with accuracy and stability at the 10^{-18} level," Nature **506**, 71–75 (2014).
6. S. M. Brewer, J.-S. Chen, A. M. Hankin, *et al.*, "$^{27}Al^+$ quantum-logic clock with a systematic uncertainty below 10^{-18}," Phys. Rev. Lett. **123**, 033201 (2019).
7. Y. Huang, B. Zhang, M. Zeng, *et al.*, "Liquid-nitrogen-cooled Ca^+ optical clock with systematic uncertainty of 3×10^{-18}," Phys. Rev. Appl. **17**, 034041 (2022).
8. A. Aeppli, K. Kim, W. Warfield, *et al.*, "Clock with 8×10^{-19} systematic uncertainty," Phys. Rev. Lett. **133**, 023401 (2024).
9. N. Dimarcq, M. Gertsvolf, G. Mileti, *et al.*, "Roadmap towards the redefinition of the second," Metrologia **61**, 012001 (2024).
10. A. D. Ludlow, M. M. Boyd, J. Ye, *et al.*, "Optical atomic clocks," Rev. Mod. Phys. **87**, 637–701 (2015).
11. M. S. Safronova, D. Budker, D. DeMille, *et al.*, "Search for new physics with atoms and molecules," Rev. Mod. Phys. **90**, 025008 (2018).
12. P. Wcisło, P. Ablewski, K. Beloy, *et al.*, "New bounds on dark matter coupling from a global network of optical atomic clocks," Sci. Adv. **4**, eaau4869 (2018).
13. R. M. Godun, P. B. R. Nisbet-Jones, J. M. Jones, *et al.*, "Frequency ratio of two optical clock transitions in $^{171}Yb^+$ and constraints on the time variation of fundamental constants," Phys. Rev. Lett. **113**, 210801 (2014).
14. N. Huntemann, B. Lipphardt, C. Tamm, *et al.*, "Improved limit on a temporal variation of m_p/m_e from comparisons of Yb^+ and Cs atomic clocks," Phys. Rev. Lett. **113**, 210802 (2014).
15. J. Grotti, S. Koller, S. Vogt, *et al.*, "Geodesy and metrology with a transportable optical clock," Nat. Phys. **14**, 437–441 (2018).
16. H. Leopardi, J. Davila-Rodriguez, F. Quinlan, *et al.*, "Single-branch Er:fiber frequency comb for precision optical metrology with 10^{-18} fractional instability," Optica **4**, 879–885 (2017).
17. N. Ohmae, N. Kuse, M. E. Fermann, *et al.*, "All-polarization-maintaining, single-port Er:fiber comb for high-stability comparison of optical lattice clocks," Appl. Phys. Express **10**, 062503 (2017).
18. H. Shi, Y. Jiang, Y. Yao, *et al.*, "Optical frequency divider: capable of measuring optical frequency ratio in 22 digits," APL Photonics **8**, 100802 (2023).
19. W. M. Itano, J. C. Bergquist, J. J. Bollinger, *et al.*, "Quantum projection noise: Population fluctuations in two-level systems," Phys. Rev. A **47**, 3554–3570 (1993).
20. G. J. Dick, "Local oscillator induced instabilities in trapped ion frequency standards," in *Proceedings of the 19th Annual Precise Time and Time Interval Systems and Applications Meeting* (1989), pp. 133–147.
21. N. Huntemann, C. Sanner, B. Lipphardt, *et al.*, "Single-ion atomic clock with 3×10^{-18} systematic uncertainty," Phys. Rev. Lett. **116**, 063001 (2016).
22. C. Sanner, N. Huntemann, R. Lange, *et al.*, "Optical clock comparison for Lorentz symmetry testing," Nature **567**, 204–208 (2019).
23. D. G. Matei, T. Legero, S. Häfner, *et al.*, "1.5 μm lasers with sub-10 mHz linewidth," Phys. Rev. Lett. **118**, 263202 (2017).
24. Boulder Atomic Clock Optical Network (BACON) Collaboration, "Frequency ratio measurements at 18-digit accuracy using an optical clock network," Nature **591**, 564–569 (2021).
25. S. Dörscher, N. Huntemann, R. Schwarz, *et al.*, "Optical frequency ratio of a $^{171}Yb^+$ single-ion clock and a ^{87}Sr lattice clock," Metrologia **58**, 015005 (2021).
26. R. Kohlhaas, A. Bertoldi, E. Cantin, *et al.*, "Phase locking a clock oscillator to a coherent atomic ensemble," Phys. Rev. X **5**, 021011 (2015).
27. J. Borregaard and A. S. Sørensen, "Efficient atomic clocks operated with several atomic ensembles," Phys. Rev. Lett. **111**, 090802 (2013).
28. T. Rosenband and D. R. Leibrandt, "Exponential scaling of clock stability with atom number," arXiv, arXiv:1303.6357 (2013).
29. T. L. Nicholson, M. J. Martin, J. R. Williams, *et al.*, "Comparison of two independent Sr optical clocks with 1×10^{-17} stability at 10^3 s," Phys. Rev. Lett. **109**, 230801 (2012).
30. M. Takamoto, T. Takano, and H. Katori, "Frequency comparison of optical lattice clocks beyond the dick limit," Nat. Photonics **5**, 288–292 (2011).
31. N. Nemitz, T. Ohkubo, M. Takamoto, *et al.*, "Frequency ratio of Yb and Sr clocks with 5×10^{-17} uncertainty at 150 seconds averaging time," Nat. Photonics **10**, 258–261 (2016).
32. E. R. Clements, M. E. Kim, K. Cui, *et al.*, "Lifetime-limited interrogation of two independent $^{27}Al^+$ clocks using correlation spectroscopy," Phys. Rev. Lett. **125**, 243602 (2020).
33. D. B. Hume and D. R. Leibrandt, "Probing beyond the laser coherence time in optical clock comparisons," Phys. Rev. A **93**, 032138 (2016).
34. X. Zheng, J. Dolde, V. Lochab, *et al.*, "Differential clock comparisons with a multiplexed optical lattice clock," Nature **602**, 425–430 (2022).
35. M. E. Kim, W. F. McGrew, N. V. Nardelli, *et al.*, "Improved interspecies optical clock comparisons through differential spectroscopy," Nat. Phys. **19**, 25–29 (2023).
36. H. Zhang, Y. Huang, B. Zhang, *et al.*, "Absolute frequency measurements with a robust, transportable $^{40}Ca^+$ optical clock," Metrologia **60**, 035004 (2023).
37. B.-K. Lu, Z. Sun, T. Yang, *et al.*, "Improved evaluation of BBR and collisional frequency shifts of NIM-Sr2 with 7.2×10^{-18} total uncertainty," Chin. Phys. Lett. **39**, 080601 (2022).
38. Bureau International des Poids et Measures, "Recommended values of standard frequencies," https://www.bipm.org/en/publications/mises-en-pratique/standard-frequencies.
39. T. Hosoya, M. Miranda, R. Inoue, *et al.*, "Injection locking of a high power ultraviolet laser diode for laser cooling of ytterbium atoms," Rev. Sci. Instrum. **86**, 073110 (2015).
40. G. Yang, H. Shi, Y. Yao, *et al.*, "Long-term frequency-stabilized optical frequency comb based on a turnkey Ti:sapphire mode-locked laser," Chin. Opt. Lett. **19**, 121405 (2021).
41. H. Telle, B. Lipphardt, and J. Stenger, "Kerr-lens, mode-locked lasers as transfer oscillators for optical frequency measurements," Appl. Phys. B **74**, 1–6 (2002).
42. E. Peik, T. Schneider, and C. Tamm, "Laser frequency stabilization to a single ion," J. Phys. B **39**, 145 (2005).
43. M. Zeng, Z. Ma, R. Hu, *et al.*, "A combined magnetic field stabilization system for improving the stability of $^{40}Ca^+$ optical clock," Chin. Phys. B **32**, 110704 (2023).

219.228.146.87 on 2024-10-31 20:41:06